December 1987 LRP 333/87

MHD STABILITY ANALYSIS FOR NET AND INTOR

F. Yasseen, W.A. Cooper, A.D. Turnbull,
F. Troyon and A. Roy

Work done under **Contract No 242/86-6/FUCH/NET**

Contract N° 242/86-6/FUCH/NET

MHD STABILITY ANALYSIS FOR NET AND INTOR

F. Yasseen,[1] W.A. Cooper, A.D. Turnbull,[2] F. Troyon and A. Roy

Centre de Recherches en Physique des Plasmas
Association Euratom / Confédération Suisse
Ecole Polytechnique Fédérale de Lausanne
21, Av. des Bains, CH-1007 Lausanne, Switzerland

ABSTRACT

The results of an MHD stability analysis of different design configurations for the NET tokamak is presented. The effect of shaping on a configuration with a moderate aspect ratio A=3.7 and elongation E=2 was investigated. The n=1 external kink stable operating windows in the q_0-q_s space have been determined at different values of β_I, for two values of the triangularity parameter δ (0.25 and 0.4). Equilibria have been generated which have, respectively, n=1 external kink mode imposed β limits of 7.6% and 7.9% or ballooning mode β limits of 8.5% and 7.8%, or that are both ballooning and kink stable at β=5.0% and 4.9%. The configuration with δ=0.4 has only a slightly wider operating window. A low aspect ratio configuration with A=1.67, E=1.68, and δ=0.3 was also studied in a similar manner but in less detail. β limits of 9.6% for the kink, 9.4% for both kink and ballooning have been obtained in this case. Finally, the problem of accessing the second region of ballooning stability for a circular cross section tokamak with A=3.7 was considered.

---

[1] Present address: Mass. Inst. of Technology, Cambridge MA 02139, USA

[2] Present address: G.A. Technologies, San Diego CA 92138, USA

A. INTRODUCTION

In this report, we concentrate on the investigation of the stable operating windows of a moderate aspect ratio A=3.7 device with elongation E=2.0 and different triangularities, δ=0.25 or δ=0.40 as a function of the plasma current, current profile, and of β_I. Such a configuration could serve as a model for the Next European Torus (NET). The stability of an alternate configuration, characterised by a low aspect ratio A=1.67, E=1.68, and δ=0.30, is also investigated, but in less detail. More specifically, the results that are presented identify the n=1 external kink stability boundaries in the q_0-q_s space, where q_0 labels the safety factor at the magnetic axis and q_s labels the safety factor at the plasma edge. The (q_0,q_s) plane is scanned by varying the current and the current profile, which can be prescribed. Different values of β_I are achieved by changing the pressure, which can also be prescribed. The pressure profile can be altered to satisfy the ballooning mode stability criterion. Finally, a circular cross section tokamak with aspect ratio A=3.7 that accesses the second region of ballooning stability is considered.

B. SHAPING EFFECTS

We first consider the effect of shaping on a moderate aspect ratio A=3.7 tokamak with elongation E=2 by investigating its stability at two values of the triangularity parameter: δ=0.25 and δ=0.40.

1. PARAMETRISATION OF THE EQUILIBRIA

The plasma-vacuum interface for the MHD equilibrium models under consideration is represented by the expressions

$$r = R + a \cos(\theta + \delta \sin\theta) \qquad (1)$$

and

$$z = E\, a \sin\theta \,, \qquad (2)$$

where r is the distance of any boundary point from the major axis and z is its distance from the midplane. The plasma shape is determined by the major radius R, the minor radius a, the elongation E, and the triangularity δ. The area S of the plasma cross-section is given by

$$S = 2\pi E a^2 \frac{J_1(\delta)}{\delta} \tag{3}$$

where J_1 is a Bessel function of the first kind. Increasing the triangularity reduces the plasma cross-section.

The average toroidal plasma current density within a poloidal magnetic flux surface ϕ is defined as

$$J(\phi) = \frac{2\pi}{V'} \int_0^{2\pi} d\theta \sqrt{g}(\vec{j}\cdot\vec{\nabla}\phi) \tag{4}$$

with

$$V'(\phi) = 2\pi \int_0^{2\pi} d\theta \sqrt{g}/r$$

where j is the plasma current density, $\sqrt{g}$ is the Jacobian, and θ and ϕ are the poloidal and toroidal angles, respectively. The total current then is

$$I = \frac{1}{2\pi} \int J(\phi) V'(\phi) d\phi .$$

Throughout this report, the current will be expressed in dimensionless form

$$I_N = \frac{\mu_o I}{aB_o} \tag{5}$$

where B_o is the value of the vacuum field at R and all quantities on the right hand side are in mks units.

The equilibria are computed using a modified version of the EQLAUS equilibrium code that allows us to prescribe together with $p'(\phi)$ the $J(\phi)$ profile instead of the covariant toroidal magnetic field $T(\phi)$ or the safety factor profile $q(\phi)$ that have characterised most previous stability investigations of tokamak devices. This procedure is better suited for optimisation studies.[1] The $J(\phi)$ profile is given by

$$J(\psi) = \left\{ \begin{array}{ll} \text{quadratic function} & 0 \leqslant \psi < \psi_a \\ \text{cubic function} & \psi_a \leqslant \psi < \psi_b \\ 0 & \psi_b \leqslant \psi < \psi_s \end{array} \right\} \quad (6)$$

where ψ is set to zero at the magnetic axis, ψ_s is the value of ψ at the plasma-vacuum interface, and the values of ψ_a and ψ_b are free parameters. The polynomials are chosen such that $J(\psi)$ and its first derivative are continuous in ψ_a and ψ_b. To reduce the number of free parameters $\psi_b - \psi_a$ is kept constant at $0.2\ \psi_s$. In the central region $J(\psi)$ is generally adjusted to keep the q profile flat. This condition has been relaxed in a few runs in order to introduce a small shear in the central region. The runs will be clearly identified.

Initially, the pressure gradient profile $p'(\psi)$ is also chosen such that its radial derivative is continuous and piecewise smooth, namely

$$p'(\psi) = \left\{ \begin{array}{ll} 0 & 0 \leqslant \psi < \psi_c \\ \text{cubic function} & \psi_c \leqslant \psi < \psi_d \\ \text{quadratic function} & \psi_d \leqslant \psi < \psi_s \end{array} \right\} \quad (7)$$

where $p'(\psi_d)$ is a maximum. The quadratic and cubic functions may thus be uniquely determined by imposing the values of $p'(\psi_d)$ and $p'(\psi_s)$. In the calculations that have been performed for the n=1 kink stability, we have fixed the value of β_I, defined as

$$\beta_I = \frac{8\pi}{\mu_0 I^2} \int p dS \quad (8)$$

and imposed $\psi_d = \psi_b$ and $\psi_c = \psi_a$. With the further condition that $J'(0) = J'(\psi_a) = 0$, we obtain a "rounded step" current profile, with the peak of the pressure gradient coinciding with the point at which $J(\psi)$ vanishes. However, in the ballooning modes study, the parametrisation of the pressure is relaxed by an equilibrium code that tailors the pressure profile so that $p'(\psi)$ satisfies the conditions of marginal stability to ballooning and Mercier modes on every ψ-surface.

A more precise and detailed description of the toroidal current and pressure profiles and the philosophy that underlies the specific

forms that are chosen for these profiles can be found in Turnbull et al.[1]

2. RESULTS

First we present the stability boundaries for the free boundary n=1 kink mode in the (q_0, q_s) space obtained using the ERATO stability code, from sequences of equilibria with the same current profile but varying total current. Such a sequence is described in Fig. 1, where the average plasma current density and pressure profiles are plotted, as well as the q-profiles corresponding to different values of the total current. Marginal stability is set at $\gamma^2 \approx 10^{-4}$, where γ is the instability growth rate normalized to an Alfvén transit time across the major radius. The density is kept constant. The results are summarized in Figs. 2 to 7.

Figure 2 shows the lowest part of the stability diagrams of the δ=0.25 configuration for 4 values of β_I in the (q_0, q_s) space. The short dashed line connects points of constant total current and varying current profile; β remains almost constant on these lines. A long dashed line in the β_I=0 diagram corresponds to a fixed current profile equilibrium sequence. Two features emerge from the comparison with the standard stability diagram of a large aspect ratio circular cross-section Tokamak: first, q_s=2 is the low q limit at β_I=0 but it increases as β_I increases while in the circular case it is at q_s=2 and independent of β; secondly, the stability window in q_0 is narrower than in the circular case and it narrows very rapidly as β_I increases. The fact that the stable region closes from the high q_0 side while the low q_0 side remains at $q_0 \approx 1$ is one feature which appears to be very general.

The same optimisation has been repeated for δ=0.40 and the results are shown in Fig. 3. There is surprising little difference in the shape and size of the stable regions. As δ increases from 0.25 to 0.40 the maximum current increases by about 10% while the width of the stable region in q_0 is only slightly increased.

In order to assess their impact on the NET design parameters, we have redrawn the operating windows for β_I=0.70, 0,95 and 1.20 shown in Figs. 2 and 3 in the (q_o, q_I) space (Fig. 4), where q_I is the cylindrical q defined as

$$q_I = \frac{2B_o S}{\mu_o I R} = \frac{2S}{aRI_N} , \qquad (9)$$

which can be rewritten with eq. 3 for the cross-sectional area as:

$$q_I = 4\pi \frac{J_1(\delta)}{\delta} \left(\frac{E}{AI_N}\right) \qquad (10)$$

Figure 4 does not show the strong influence on δ that is expected from previous studies.[2] There is only a slightly larger stability window at high β_I. Note that q_{Imin} is substantially below 2 rising almost proportionally to β_I in the range of β_I considered.

The β_I=0 eigenstructures for equilibria with δ=0.4 at three unstable points of Fig. 3 are displayed in Figs. 5, 6 and 7. The flow pattern in Fig. 5 corresponds to an equilibrium with q_0<1 and q_S>2 and is typical of an n=1 toroidal kink.[3] The equilibrium in Fig. 6 has $1.0<q_0<1.5$ and q_S<2 and the flow pattern corresponds to an m=2, n=1 external kink mode. The third equilibrium, shown in Fig. 7, is strongly unstable and lies in the region $1.35<q_0<2$ and q_S<3. The eigenstructure observed is more or less characteristic of an m=2, n=1 mode with activity localised around the q=2 surface.

We have also performed random checks for the n=2 kink mode at β_I=0.95 for both triangularities. This does not seem to noticeably alter the stability domain.

The highest values for the n=1 kink mode imposed β limit that we have obtained by scanning the (q_0, q_S) plane at fixed values of β_I are β=7.6% for δ=0.25 at β_I=1.2 and I=2.33, and β=7.9% for δ=0.4 at the same β_I and I=2.37. In Fig. 10, labeled as kink, the results

shown in Figs. 2 nd 3 are cross-plotted in the (β,q_o) plane. The maximum value of β is not well determined because of the narrowness in q_o of the operating region. Compared to the optimisation we have done for NET[4] and JET[5] these stability windows are much more narrow but the maximum values of β are higher than those found in these studies at the same normalized current I_N. There is no evidence of a dependence on the triangularity for these high current, low q_I configurations.

The equilibria described so far are ballooning unstable in the edge regions at β much below the maximum kink stable β, and Mercier unstable in the low shear region where the current density just starts to drop. We have optimized some of these equilibria using a code developed by A. Roy, which combines EQLAUS and ERATO, and which adjusts iteratively the pressure profile until $p'(\phi)$ satisfies the ballooning and Mercier marginal stability criteria on every ϕ-surface, keeping the current density $J(\phi)$ unchanged. The kink stability is not much affected since q_o does not change much and this small change can be accommodated with a slight change of the current width. The result is a sharp decrease of β by 30-40%. The introduction of a small amount of shear in the central region has been found to improve the ballooning limit. An example of such an equilibria is shown in Fig. 9 which is fully stable at β=5%. Note that there is little pressure gradient in the region $J\neq0$. There has not been an extensive study to optimize the current profile. The reason for the improvement of β is not obvious: The shear in the edge region has been slightly reduced which is expected to reduce rather than increase the β in the first region of stability and there is too little shear in the central region to make a measurable contribution to the β. It may be the same effect as found by C.M. Bishop et al.[6], namely that $J\neq0$ in the outer region increases the ballooning limit.

The same ballooning optimisation has ben repeated for the same current profiles as for the n=1 optimisation, with a slight adjustment in the central region when found profitable. The result is shown in Figs. 10 and 11. Compared to the n=1 kink limit the balloning limit is reduced substantially. For this class of equilibria the ballooning criterion is more stringent than the kink limit.

Figure 11 shows that the β limit obtained is as good as could be expected but the linear dependence on I_N is not correct in this range of current.

Since a wider current profile is good for ballooning stability we have made some attempts at improving the ballooning limit by increasing q_0 at reduced current to obtain steep q profiles at the edge. For δ=0.25 and 0.4 we have obtained ballooning stable equilibria with β=8.5% and 7.8% respectively at the same normalized current I_N=1.85. Figure 12 shows the profiles of current density, pressure and safety factor for the first of these equilibria. This optimisation shows again a surprising lack of sensitivity of the limiting β on triangularity.

3. CONCLUSIONS

For reference we note that the NET extended configuration with I=15MA, B=4.8T, R=5.2m, a=1.70m has a normalized current of I_N=2.30 which falls in the range of values studied. The stability analysis presented shows that at such a current the plasma can be stable to the n=1 external kink up to β of the order of 7%, but the operating range is becoming very narrow in q_0 at high β. Ballooning stability appears to be more stringent, limiting β to less than 5%, but this may not be the final answer as there appears possible to make some trade off between the n=1 kink limit and the ballooning limit by widening the current profile, keeping q_0 constant. Another possibility would be to introduce a higher multipolar deformation of the surface which could increase the ballooning limit, since the pressure gradient is concentrated at the edge and sensitive to the shape of the surface, without affecting the kink limit.

The lack of sensitivity of the β limit on the triangularity is surprising and more studies over a wider domain are clearly needed. The insensitivity of β_{max} on the current I_N is also surprising and the range of I_N should be extended. Lower I_N implies higher q_s which makes such studies very difficult and costly because of the high resolution needed in ERATO.

C. LOW ASPECT RATIO CONFIGURATION

We now investigate the stability properties of a low aspect ratio configuration, in the same way as in the preceding section, but in less detail. This configuration is characterized by A=1.67, E=1.68, and δ=0.30.

RESULTS

The n=1 kink mode stability boundaries for the low aspect ratio design are displayed in Fig. 13 (at zero β_I) (at β_I=0.35). The stable domains in both cases have the shape of two stalactites with a weakly unstable stalagmite wedged in between, and centered at $q_0 \simeq 1.05$. This unstable wedge is due to off-resonant m=1 modes driven by the toroidal coupling in the low shear region of the plasma. These modes do not appear for A=3.7, since the toroidal coupling is weaker. They are stabilized by increasing the shear near the magnetic axis. This can be achieved (as mentioned earlier) by peaking the current density profile at the center and rounding off its edge. As previously seen, we also find that increasing β_I raises the smallest stable q_s, and reduces the stable domain.

The highest value found for the n=1 kink imposed β limit was 9.6%, at I_N=5.73. With the ballooning optimisation code, we have obtained a promising equilibrium that is characterised by a peaked pressure profile. It can be used to generate a sequence of different equilibria at different currents. At I_N=3.67, the equilibrium is both kink and ballooning stable with β=9.4% (c.f. Fig. 14). Due to the peaked pressure profile, it is Mercier unstable in a very small region around the magnetic axis. However, this region is so small that one should achieve stability without affecting β by shaving off the pressure profile in this region. These results are included in Table 1.

The operating window shown in Fig. 13 has been redrawn in q_0-q_I space (Fig. 15). In this case $q_I^{min} \simeq 1.1$. This decrease in the value of q_I^{min} must be a consequence of the low aspect ratio.

D. SECOND BALLOONING STABLE REGIME

Circular cross section Tokamak with aspect ratio 3.7 that access the second stable region of ballooning modes are investigated in this section. The MHD equilibria are obtained with the VMEC inverse moments equilibrium code,[7] and mapped to straight magnetic field line coordinates for the ballooning stability analysis. The safety factor profile is parametrised by $1/q=1/q_0+(1/q_s-1/q_0)\Phi^4$, where Φ is the toroidal magnetic flux function. The example we investigate has $q_0=1.25$, $q_s=3.846$ and is shown in Fig. 16. Flux conserving sequences of equilibria are obtained that attempt to optimise the pressure profile to achieve marginal stability conditions to ballooning modes on all the flux surfaces. The pressure profile for a case with $\beta=7.15\%$ is shown in Fig. 17. The surfaces with $\Phi<0.3$ and $\Phi\geq 0.6$ are marginally stable. However, for $0.3<\Phi<0.6$ the plasma is strongly stable in the second regime.The stability properties of the $\beta=7.15\%$ equilibrium we have generated are insensitive to variation of the radial wave number because the second stable region, as well as the inner first stable region, are within the domain of weak global shear. Increasing the pressure gradient further in the stable domain causes the inner second stable surfaces to return back into the first stability region. On the other hand, surfaces in the vicinity of the outer boundary of the second stable region that were previously marginal become strongly stable and incorporated in that domain. As a consequence, a higher value of β is obtained. However, for β values in excess of the 7.15% we have reported, we have experienced convergence problems with the equilibrium calculation that result from the large local change of pressure gradient near the second stable region inner and outer boundaries that cannot be adequately resolved with the 41 point radial mesh we have utilised. It should be noted that a similar calculation with $q_0=1.05$ failed to produce a fully stable plasma with $\beta>4\%$.

REFERENCES

[1] A.D. Turnbull, M.A. Secrétan, F. Troyon, S. Semenzato and R. Gruber, J. Comput. Phys. 66, 391 (1986).

[2] A.M.M. Todd et al., Nucl. Fusion 19, 743 (1979).

[3] A.D. Turnbull and F. Troyon, Proc. 12th Europ. Conf. on Contr. Fusion and Plasma Phys., Budapest, Sept 1985, Europhysics Abstracts, Suppl. to the Proceedings Part I, 48-51 (1985).

[4] F. Troyon et al., NET Report, EURXII-324/14, Brussels.

[5] H. Saurenmann et al., LRP 263/85.

[6] C.M. Bishop et al., Nucl. Fusion 26, 1063 (1986).

[7] S.P. Hirshman, U. Schwenn and J. Nuehrenberg, Comput. Phys. Comm. (to be published).

ACKNOWLEDGMENT

Useful discussions with Dr. T. Tsunematsu are gratefully ackowledged.

FIGURE CAPTIONS

Fig. 1: The average plasma current density, safety factor q, and pressure profiles with $\psi_a/\psi_s=0.60$ and $\psi_b/\psi_s=0.80$ from a typical equilibrium at $\beta_I=0.70$ for $\delta=0.40$, $E=2.00$ and $A=3.7$. The equilibrium is characterised by the normalised current $I_N=2.59$, $\beta=5.3\%$ and $(q_0, q_s)=(0.954, 2.98)$. It is marginally stable to the n=1 kink mode. The segments in the top right hand corner indicate the surfaces which are ballooning or Mercier unstable. Also plotted are the q-profiles corresponding to equilibria from the same sequence obtained for $I_N=2.04$ and $I_N=1.67$.

Fig. 2: The n=1 stability boundaries in the (q_0, q_s) space for a configuration with $\delta=0.25$, $E=2.0$ and $A=3.7$ (solid curve) and increasing β_I : 0, 0.7, 0.95 and 1.20. The long dashed lines at $\beta_I=0$ identify sequences of equilibria with fixed average current density profile. The short dashed lines connect points that have the same normalised total current I_N.

Fig. 3: The n=1 stability boundaries in the (q_0, q_s) space for a configuration with $\delta=0.40$, $E=2.0$ and $A=3.7$ (solid curve) for the same values of β_I = 0, 0.7, 0.95 and 1.20 as in Fig. 2.

Fig. 4: The stability boundaries in the (q_0, q_I) space at $\beta_I=0.70$, 0.95 and 1.20 for configurations with $A=3.7$, $E=2.00$, and $\delta=0.4$ (dashed curves) or $\delta=0.25$ (solid curves).

Fig. 5: The n=1 instability flow pattern in a configuration with $E=2.0$, $A=3.7$, $\delta=0.4$ and $\beta=0$. The equilibrium state has $q_0=0.92$ and $q_s=3.14$.

Fig. 6: The n=1 instability flow pattern in a configuration with $E=2.0$, $A=3.7$, $\delta=0.4$ and $\beta=0$. The equilibrium state has $q_0=1.23$ and $q_s=1.99$.

Fig. 7: The n=1 instability flow pattern in a configuration with E=2.0, A=3.7, δ=0.4 and β=0. The equilibrium state has q_0=1.37 and q_S=2.27.

Fig. 8: The average plasma current density, pressure and safety factor profiles for an n=1 kink stable equilibrium with δ=0.4, E=2.00, A=3.7 and I_N=2.37 at β_I=1.20. This equilibrium is characterised by q_0=1.0, q_S=3.47, and yields β=7.9%. The ballooning and Mercier unstable surfaces are indicated by the segment in the top right hand side.

Fig. 9: The average plasma current density, pressure and safety factor profiles for a stable equilibrium to both kink and ballooning, with δ=0.25, E=2.00, A=3.7, I_N=2.00 at β_I=1.06. This equilibrium is characterised by q_0=0.97, q_S=3.70, and has β=5.0%. In this case, the current profile is slightly peaked at the magnetic axis.

Fig. 10: The β stable windows at currents I_N=2.22 (top), I_N=2.405, (middle), and I_N=2.59 (bottom), for configurations with A=3.7, E=2.00, and δ=0.25 (LHS) or δ=0.4 (RHS). The dashed line indicates the n=1 kink imposed limits. The continuous line indicates the ballooning imposed limits.

Fig. 11: The average plasma current density, pressure and safety factor profiles for a ballooning stable (but n=1 kink unstable) equilibrium with δ=0.25, E=2.0, A=3.7, I_N=1.85 and β_I=1.98. This equilibrium is characterised by q_0=1.56, q_S=3.56, and yields β=8.5%.

Fig. 12: The limiting values of β as a function of I_N for two configurations with E=2.00, A=3.70 and different triangularities: δ=0.25 and δ=0.40. The crosses indicate the values that are stable to the n=1 kink only and the asterisks indicate values that are stable to both kink and ballooning.

Fig. 13: The $\beta_I=0$, $\beta_I=0.35$ n=1 stability boundaries in the (q_0, q_S) space for a configuration with $\delta=0.30$, E=1.68 and A=1.67 (solid curve). The short dashed lines connect points that have the same normalised current I_N. The dashed-dotted lines surround a weakly unstable area.

Fig. 14: The average plasma current density, pressure and safety factor profiles for a ballooning and n=1 kink stable equilibrium with $\delta=0.30$, E=1.68, A=1.67, $I_N=3.67$ and $\beta_I=0.613$. This equilibrium is characterised by $q_0=1.19$, $q_S=4.9$, and yields $\beta=9.4\%$. The plasma is weakly Mercier unstable in a small region $\phi/\psi_S<0.01$.

Fig. 15: The $\beta_I=0.35$ n=1 stability boundary in the (q_0, q_I) space for the same configuration as in Fig. 13: $\delta=0.30$, E=1.68 and A=1.67 (solid curve).

Fig. 16: The dependence of the safety factor q on the toroidal flux Φ, assumed in the study of the second ballooning stable regime for a circular cross-section device with A=3.7.

Fig. 17: Pressure profile of a ballooning stable equilibrium that has $\beta=7.15\%$ for a circular cross-section device with A=3.7. The region within $0.30<\Phi<0.60$ lies in the second stable regime.

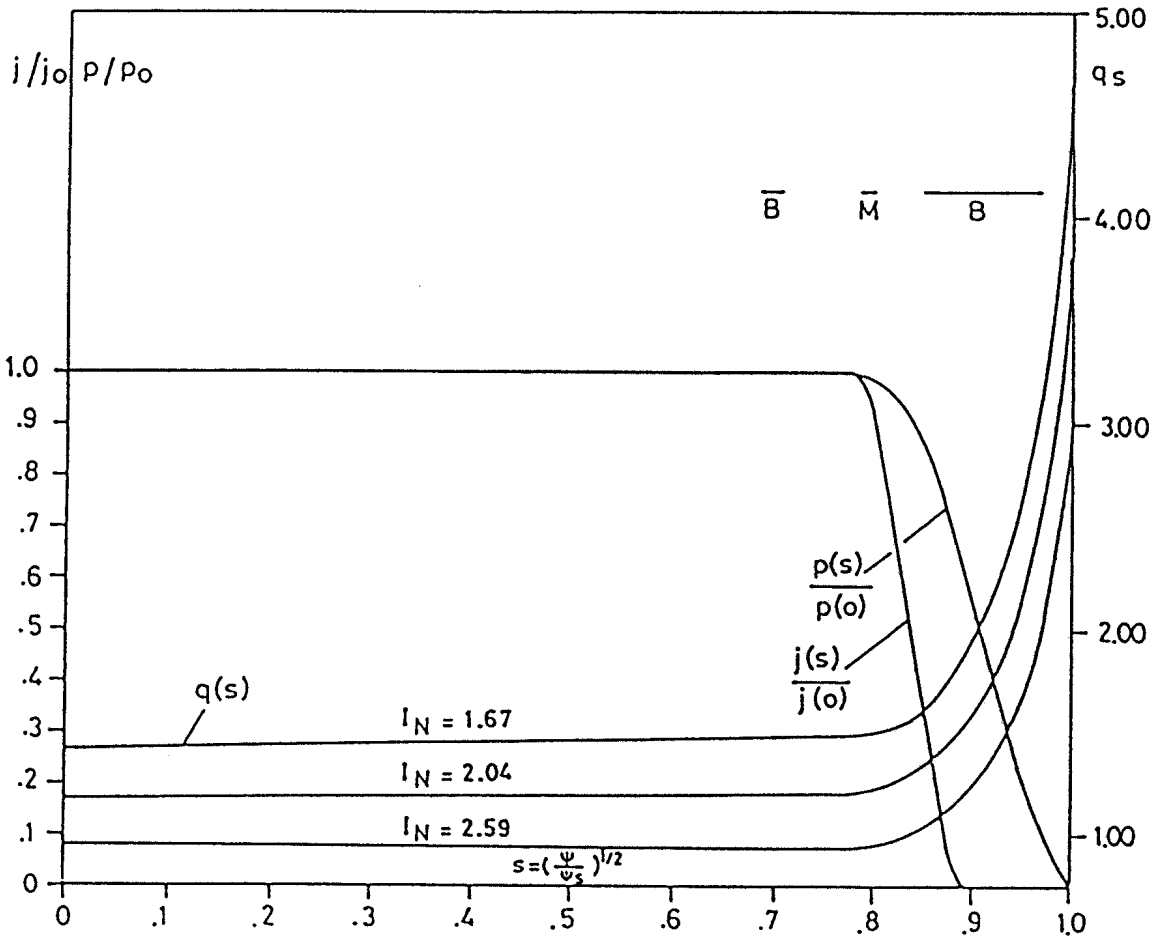
j/jo p/po
qs
5.00
4.00
3.00
2.00
1.00
B̄ M̄ B̄
1.0
.9
.8
.7
.6
.5
.4
.3
.2
.1
0
p(s)/p(o)
j(s)/j(o)
q(s)
I_N = 1.67
I_N = 2.04
I_N = 2.59
s=(ψ/ψs)^1/2
0 .1 .2 .3 .4 .5 .6 .7 .8 .9 1.0

FIG. 1

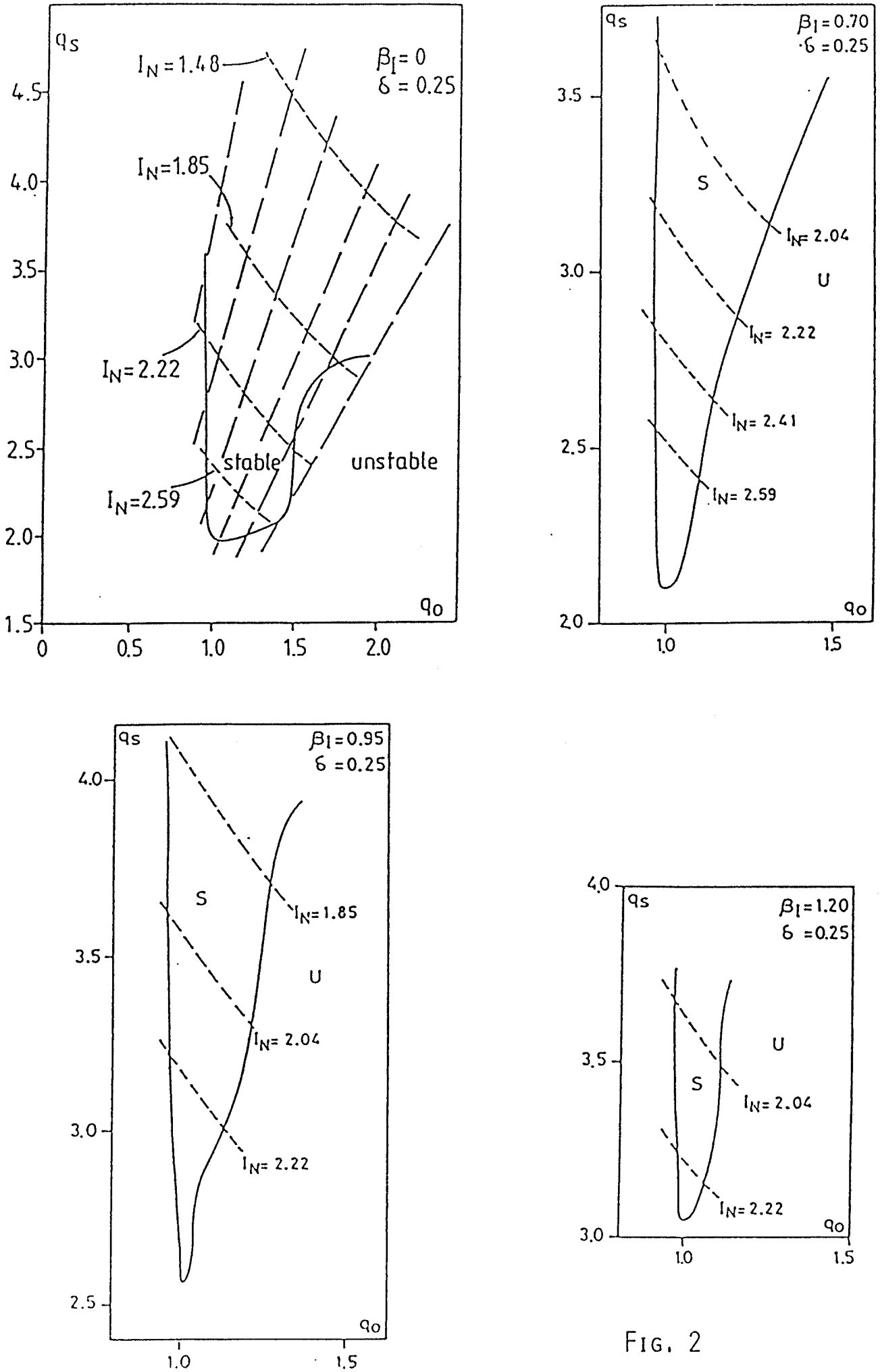
qs
$I_N = 1.48$
$\beta_I = 0$
$\delta = 0.25$
$I_N = 1.85$
$I_N = 2.22$
stable
unstable
$I_N = 2.59$
qo
4.5
4.0
3.5
3.0
2.5
2.0
1.5
0
0.5
1.0
1.5
2.0
qs
$\beta_I = 0.70$
$\delta = 0.25$
S
U
$I_N = 2.04$
$I_N = 2.22$
$I_N = 2.41$
$I_N = 2.59$
qo
3.5
3.0
2.5
2.0
1.0
1.5
qs
$\beta_I = 0.95$
$\delta = 0.25$
S
U
$I_N = 1.85$
$I_N = 2.04$
$I_N = 2.22$
qo
4.0
3.5
3.0
2.5
1.0
1.5
qs
$\beta_I = 1.20$
$\delta = 0.25$
S
U
$I_N = 2.04$
$I_N = 2.22$
qo
4.0
3.5
3.0
1.0
1.5

FIG. 2

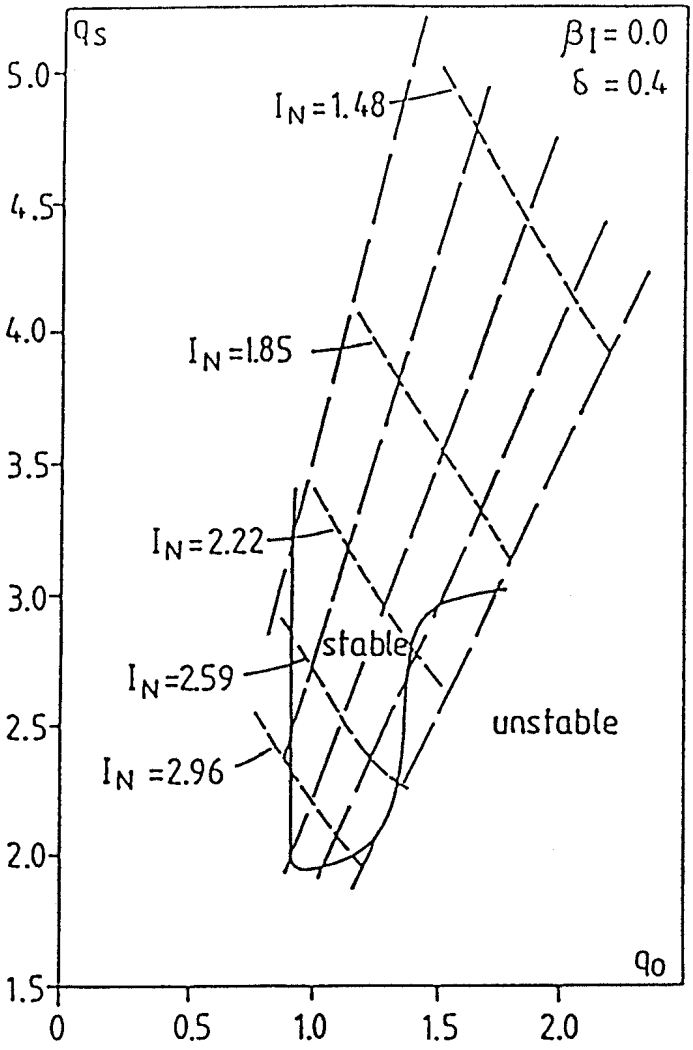
qs
βI = 0.0
δ = 0.4
IN = 1.48
IN = 1.85
IN = 2.22
IN = 2.59
IN = 2.96
stable
unstable
q0
5.0
4.5
4.0
3.5
3.0
2.5
2.0
1.5
0
0.5
1.0
1.5
2.0

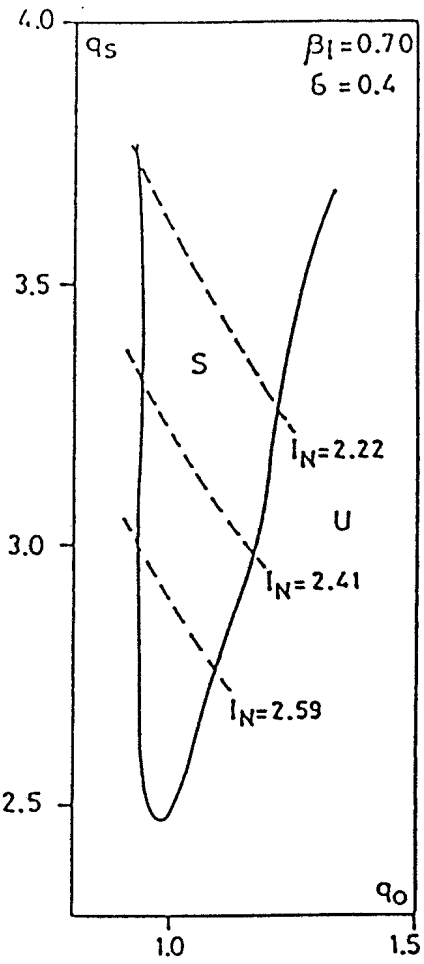
qs
βI = 0.70
δ = 0.4
S
U
IN = 2.22
IN = 2.41
IN = 2.59
q0
4.0
3.5
3.0
2.5
1.0
1.5

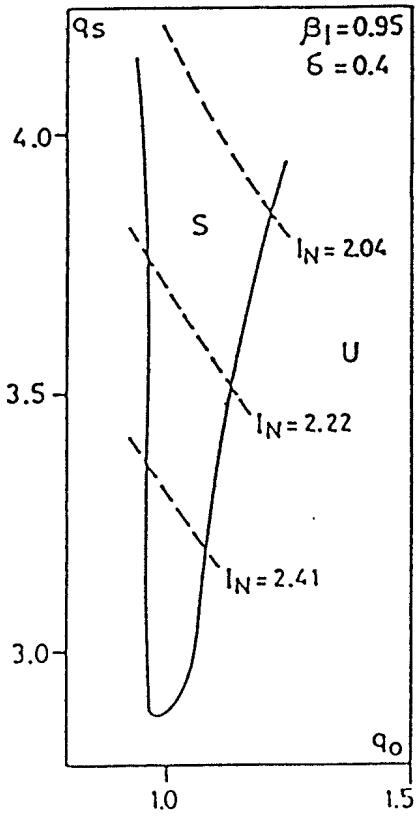
qs
βI = 0.95
δ = 0.4
S
U
IN = 2.04
IN = 2.22
IN = 2.41
q0
4.0
3.5
3.0
1.0
1.5

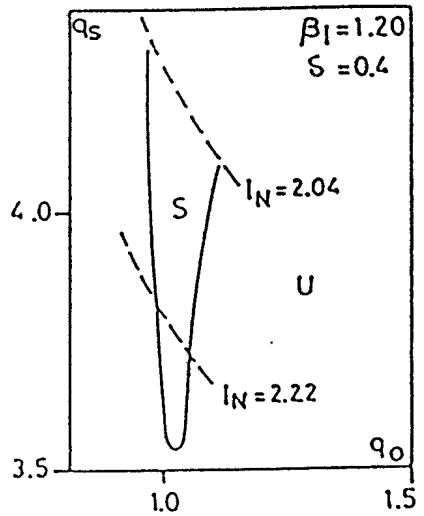
qs
βI = 1.20
δ = 0.4
S
U
IN = 2.04
IN = 2.22
q0
4.0
3.5
1.0
1.5

FIG. 3

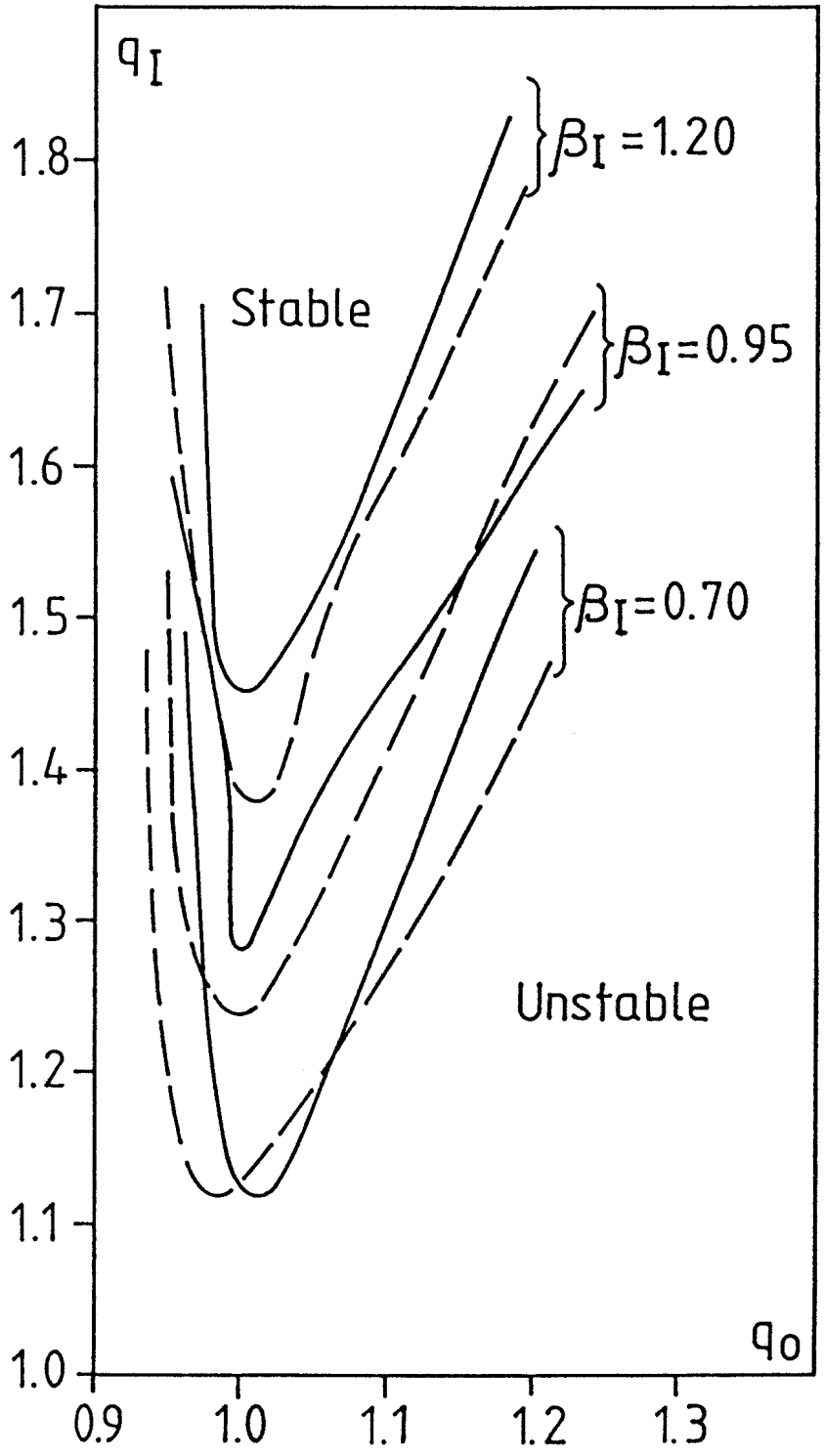
q_I
$\beta_I = 1.20$
$\beta_I = 0.95$
$\beta_I = 0.70$
Stable
Unstable
q_o
1.8
1.7
1.6
1.5
1.4
1.3
1.2
1.1
1.0
0.9
1.0
1.1
1.2
1.3

FIG. 4

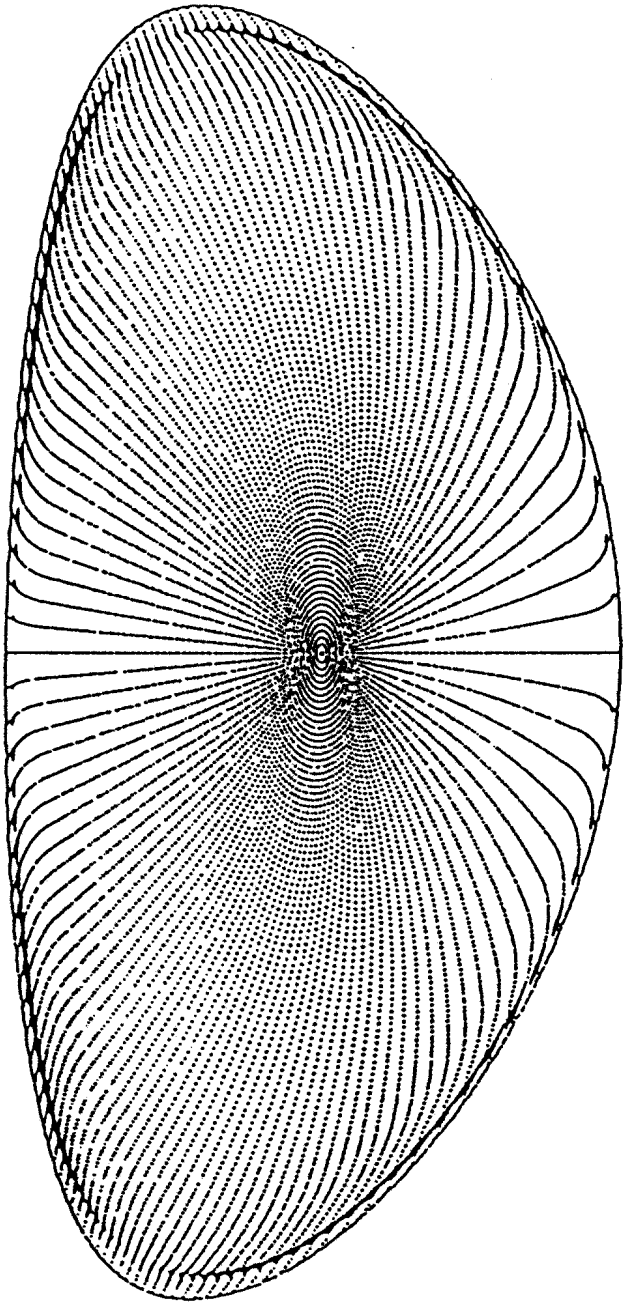

FIG. 5

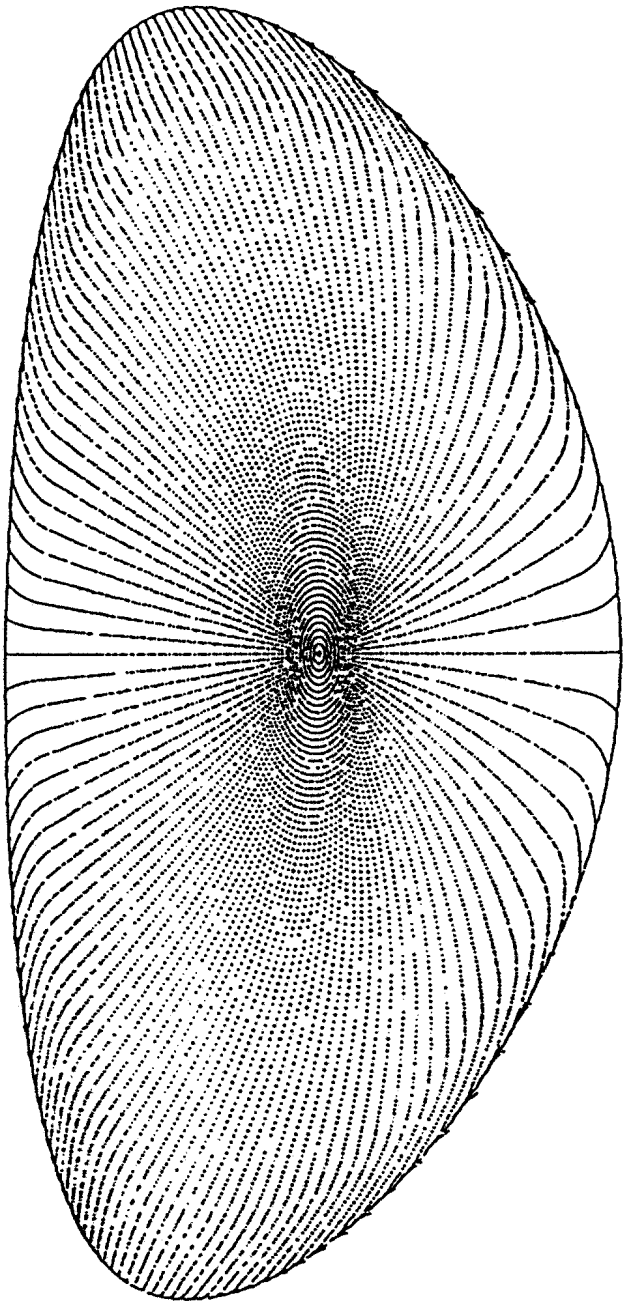

FIG. 6

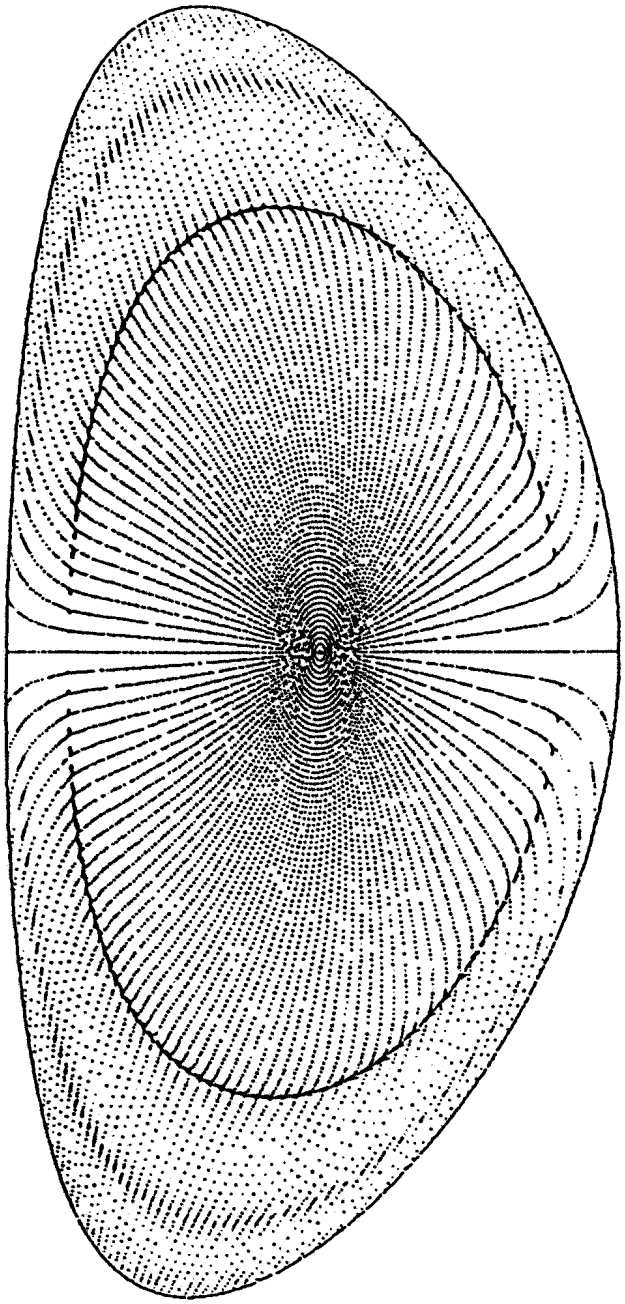

FIG. 7

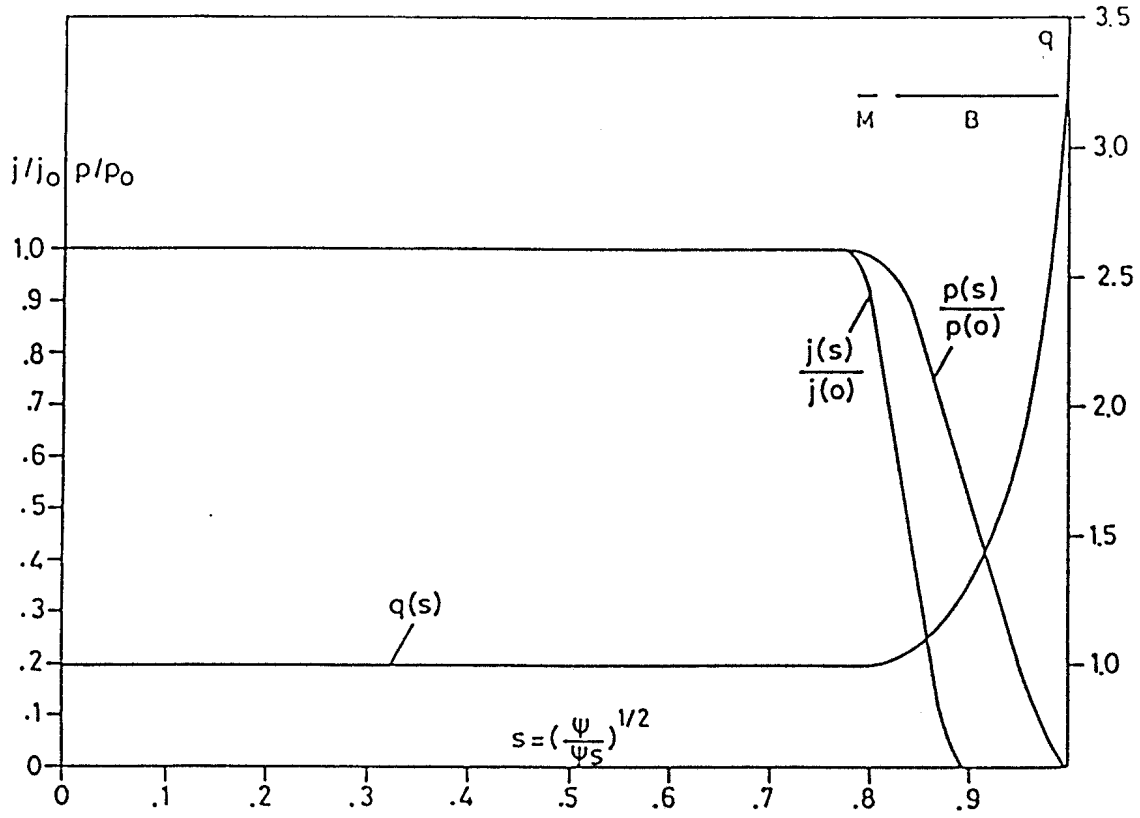
q
M
B
j/j₀ p/p₀
1.0
.9
.8
.7
.6
.5
.4
.3
.2
.1
0
3.5
3.0
2.5
2.0
1.5
1.0
p(s)/p(o)
j(s)/j(o)
q(s)
s=(ψ/ψs)^1/2
0
.1
.2
.3
.4
.5
.6
.7
.8
.9

FIG. 8

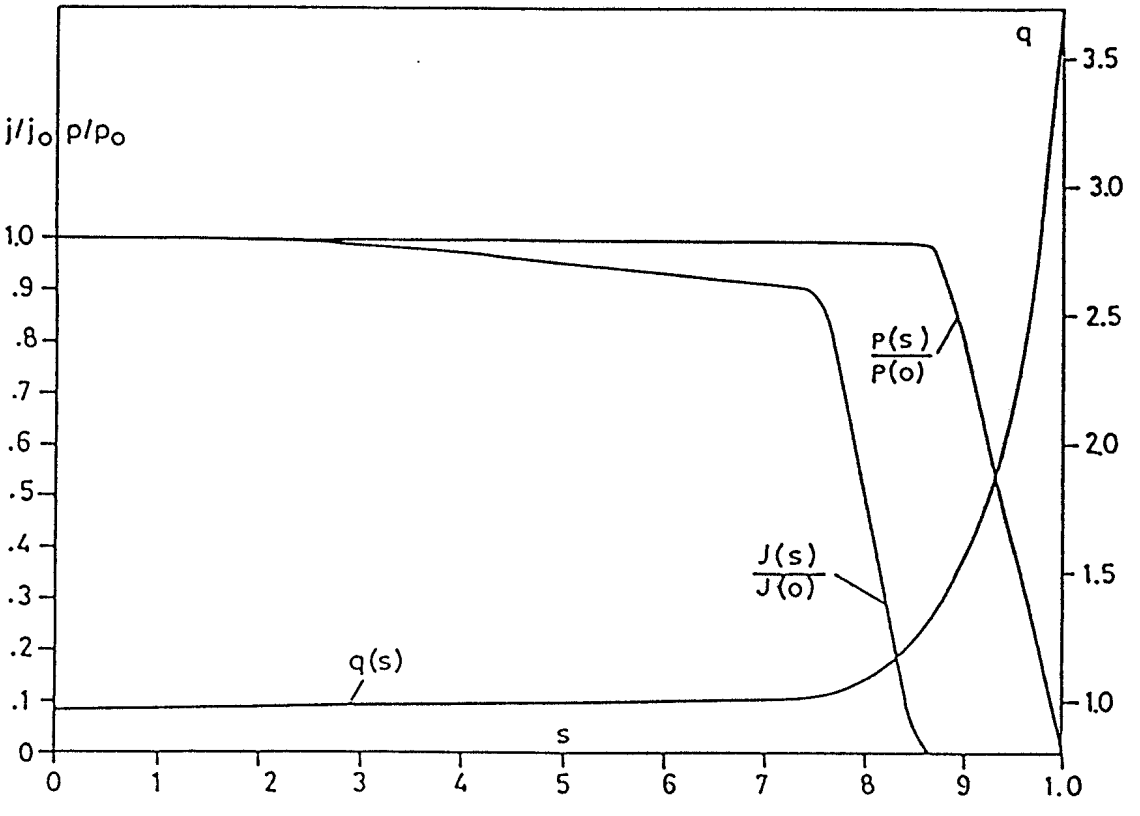
q
j/j₀ p/p₀
1.0
.9
.8
.7
.6
.5
.4
.3
.2
.1
0
3.5
3.0
2.5
2.0
1.5
1.0
P(s)/P(o)
J(s)/J(o)
q(s)
s
0
1
2
3
4
5
6
7
8
9
1.0

FIG. 9

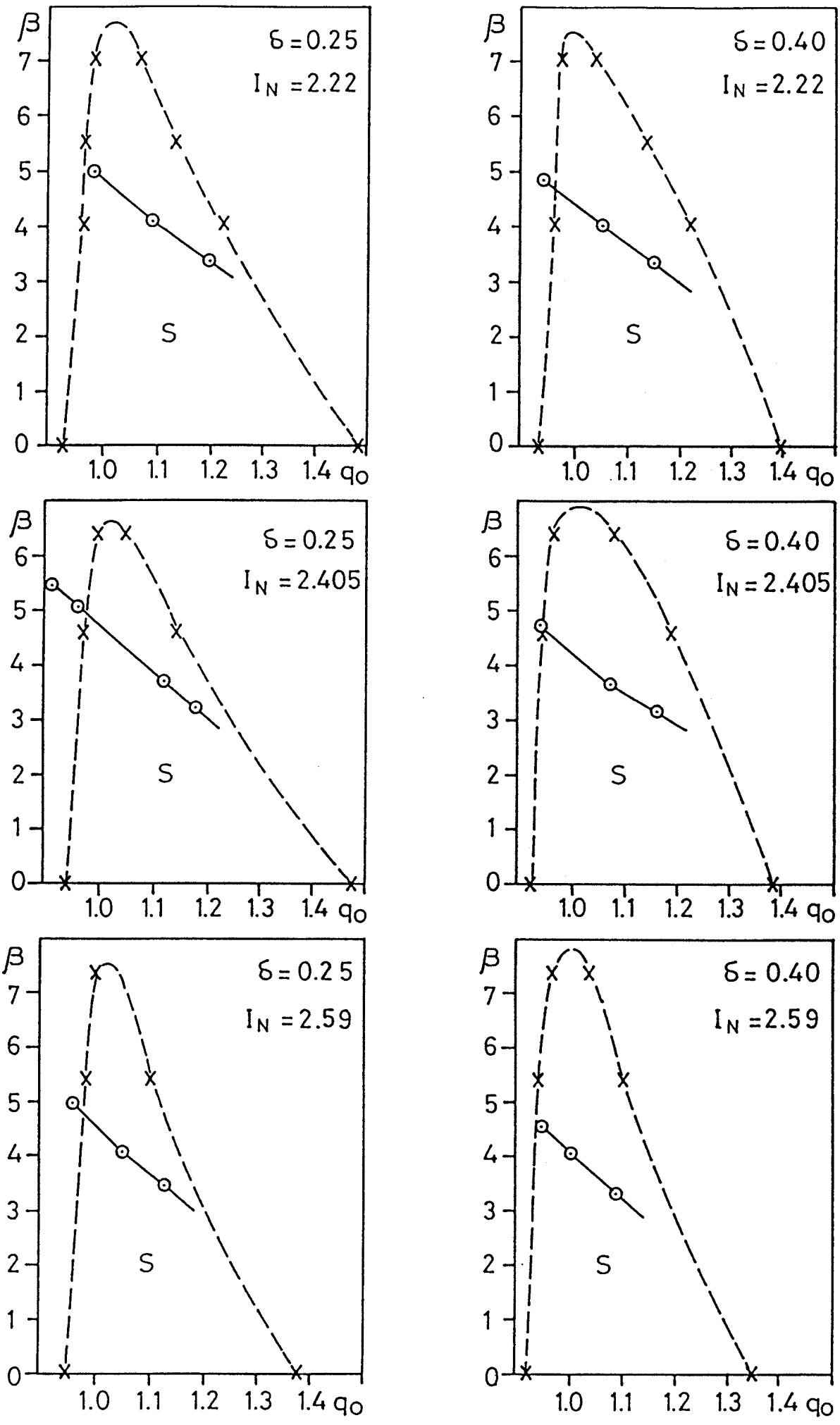
β
δ = 0.25
I_N = 2.22
S
1.0 1.1 1.2 1.3 1.4 q_o
δ = 0.40
I_N = 2.22
δ = 0.25
I_N = 2.405
δ = 0.40
I_N = 2.405
δ = 0.25
I_N = 2.59
δ = 0.40
I_N = 2.59

FIG. 10

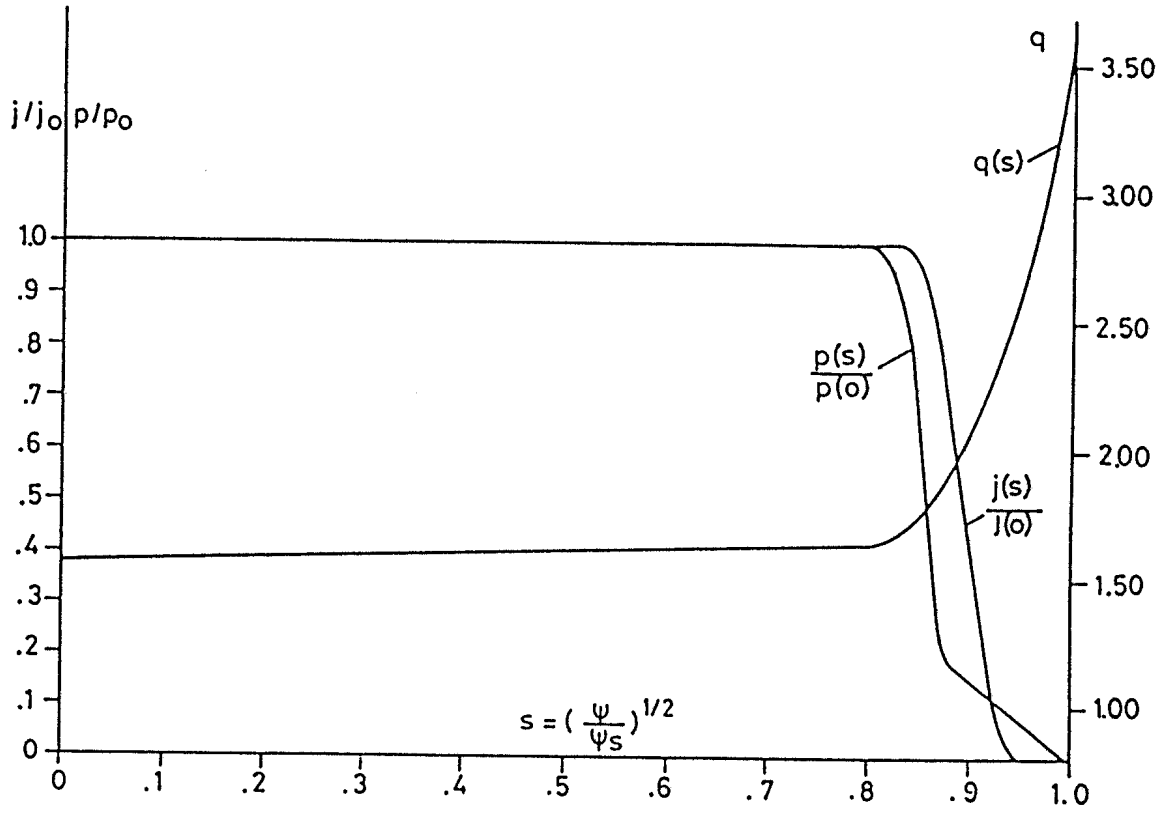
j/j₀ p/p₀
q
3.50
3.00
2.50
2.00
1.50
1.00
q(s)
p(s)/p(0)
j(s)/j(0)
1.0
.9
.8
.7
.6
.5
.4
.3
.2
.1
0
s = (ψ/ψs)^1/2
0
.1
.2
.3
.4
.5
.6
.7
.8
.9
1.0

FIG. 11

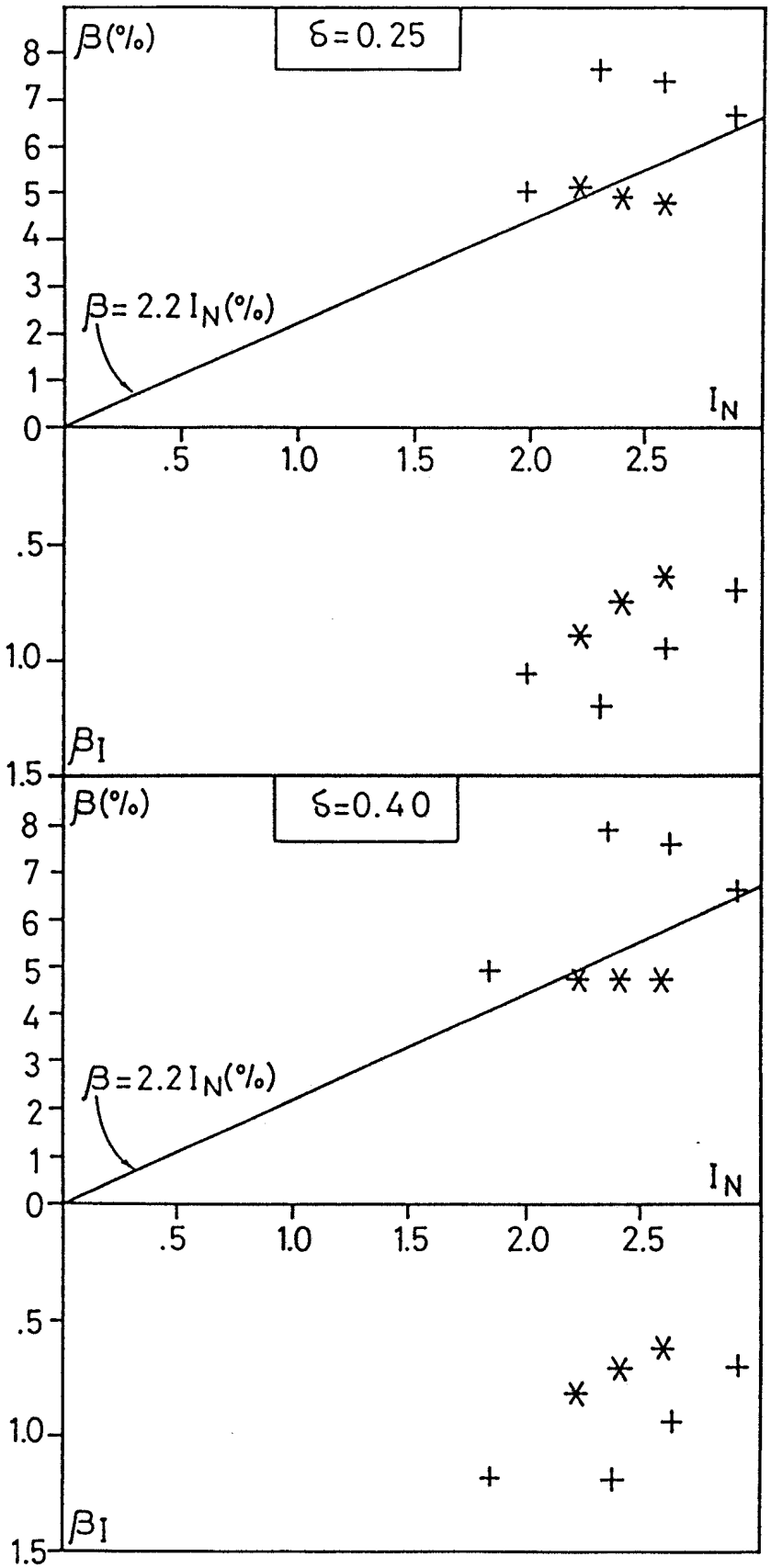

FIG. 12

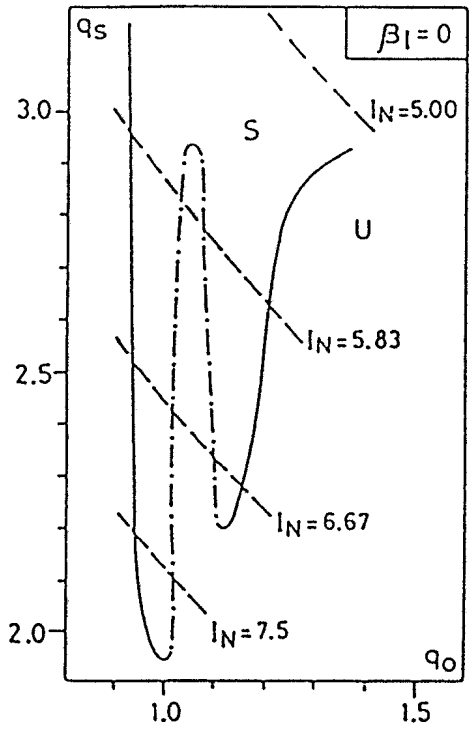
qs
βI = 0
IN=5.00
S
U
IN=5.83
IN=6.67
IN=7.5
3.0
2.5
2.0
qo
1.0
1.5

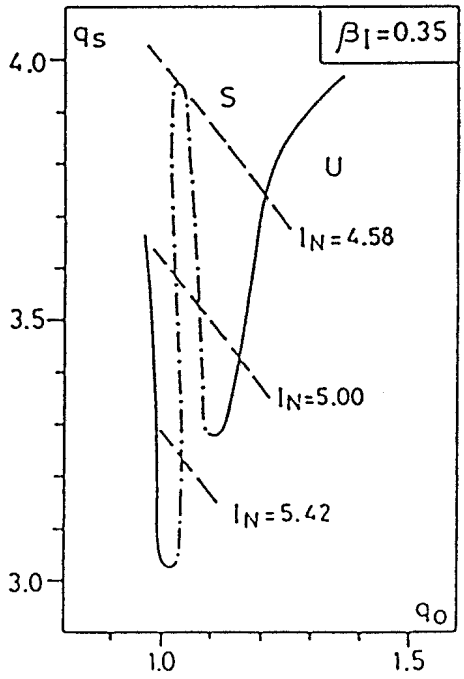
qs
βI=0.35
S
U
IN=4.58
IN=5.00
IN=5.42
4.0
3.5
3.0
qo
1.0
1.5

FIG. 13

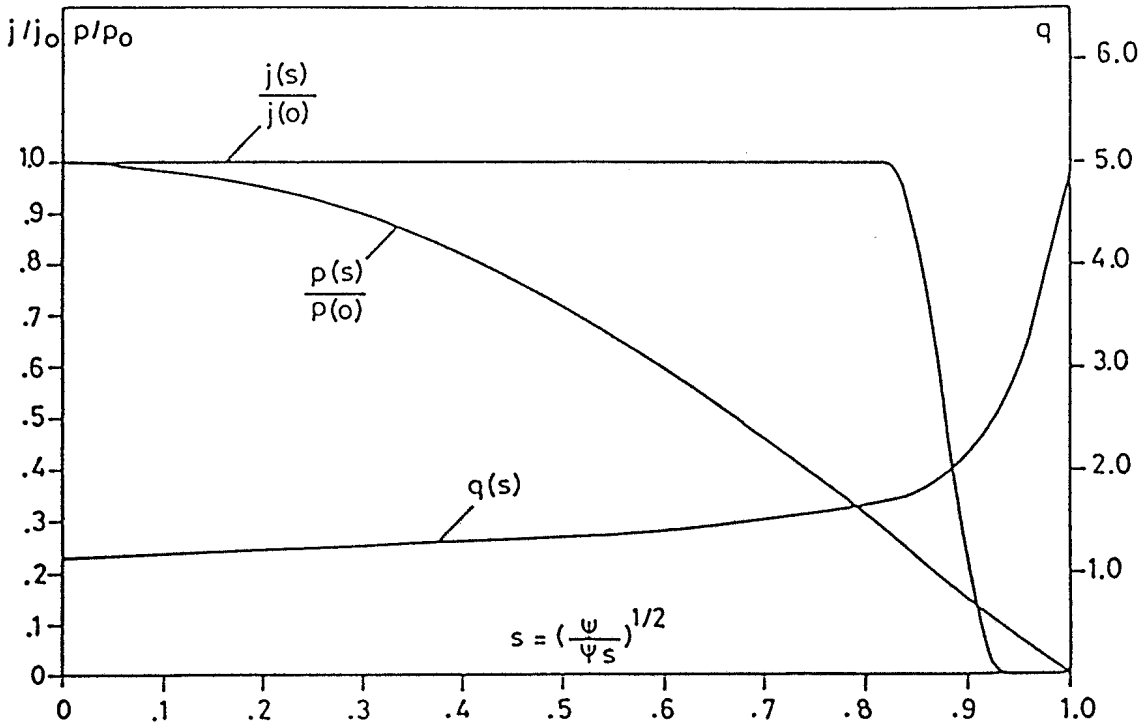
j/j₀ p/p₀
q
j(s)/j(o)
p(s)/p(o)
q(s)
s = (ψ/ψs)^1/2
1.0
.9
.8
.7
.6
.5
.4
.3
.2
.1
0
6.0
5.0
4.0
3.0
2.0
1.0
0
.1
.2
.3
.4
.5
.6
.7
.8
.9
1.0

FIG. 14

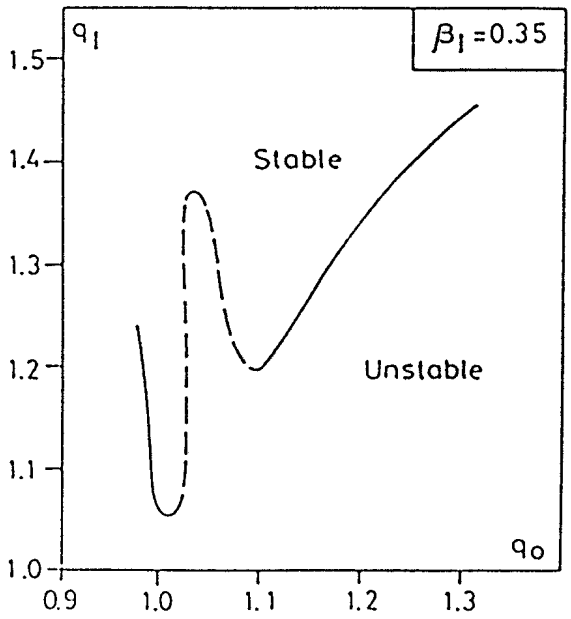
q₁
β₁ = 0.35
Stable
Unstable
q₀
1.5
1.4
1.3
1.2
1.1
1.0
0.9
1.0
1.1
1.2
1.3

FIG. 15

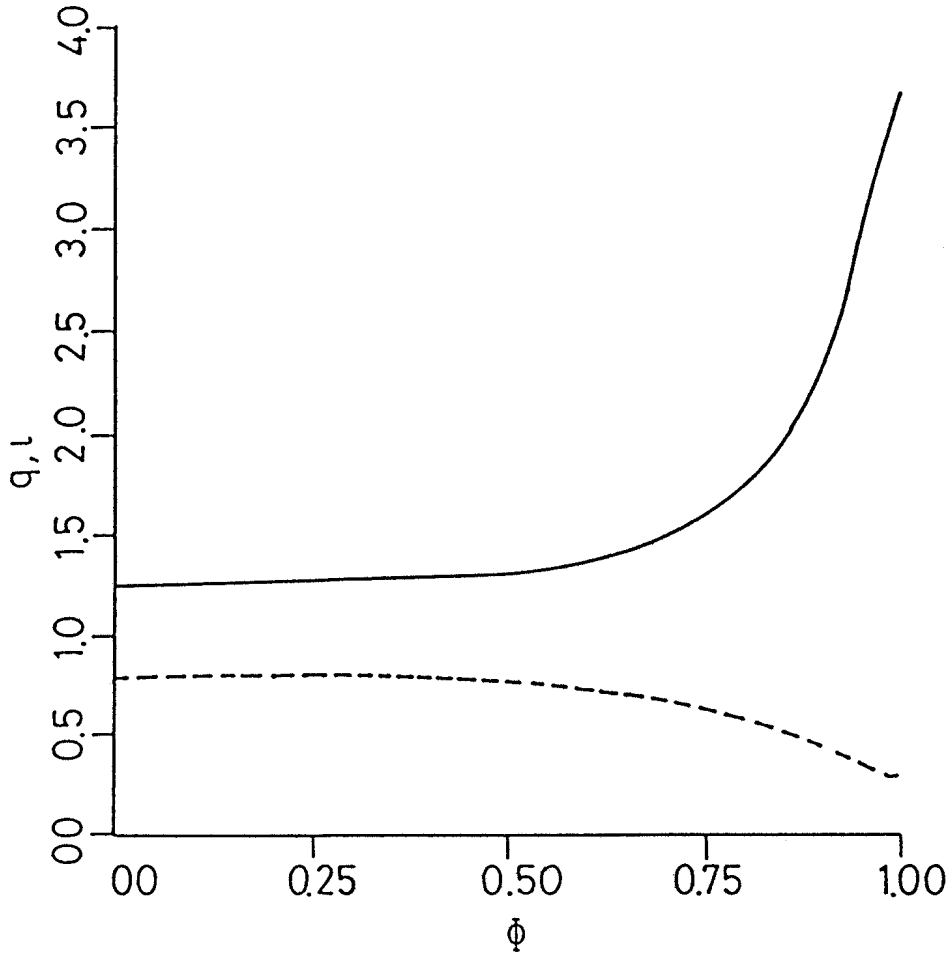

FIG. 16

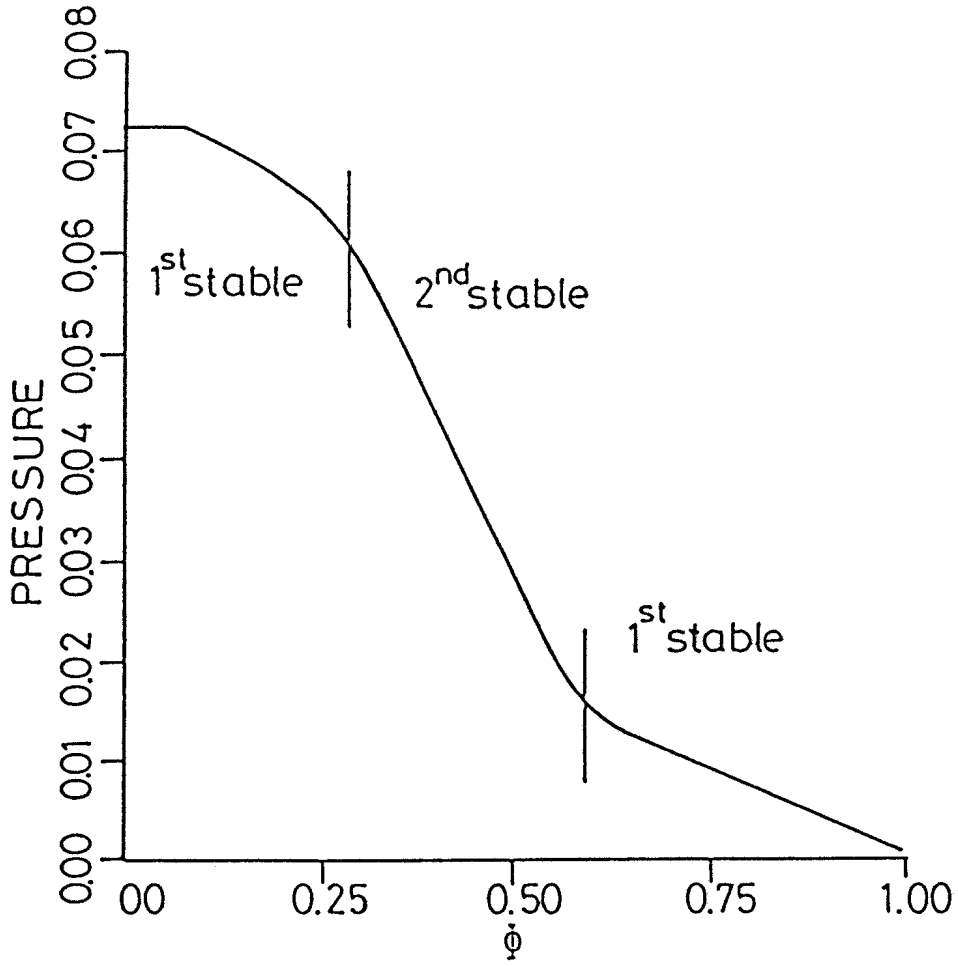
PRESSURE
0.00
0.01
0.02
0.03
0.04
0.05
0.06
0.07
0.08
1st stable
2nd stable
1st stable
00
0.25
0.50
0.75
1.00
Φ

FIG. 17